American Journal of Pathology, Vol. 164, No. 5, May 2004


# Tissue Distribution, Biochemical Properties, and Transmission of Mouse Type A AApoAII Amyloid Fibrils

Tatsumi Korenaga,* Xiaoying Fu,* Yanming Xing,* Takatoshi Matsusita,† Kazunao Kuramoto,‡ Seigo Syumiya,‡ Kazuhiro Hasegawa,§ Hironobu Naiki,§ Masaki Ueno,¶ Tokuhiro Ishihara,‖ Masanori Hosokawa,** Masayuki Mori,* and Keiichi Higuchi*

*From the Department of Aging Biology,* Institute on Aging and Adaptation, Shinshu University Graduate School of Medicine, Matsumoto; the Field of Regeneration Control,† Institute for Frontier Medical Science, Kyoto University, Kyoto; the Laboratory Animal Facilities,‡ Tokyo Metropolitan Institute of Gerontology, Tokyo; the Department of Pathology,§ Fukui Medical University, Matsuoka; the Department of Inflammation Pathology,¶ Kagawa Medical University, Miki; the First Department of Pathology,‖ Yamaguchi University School of Medicine, Ube; and the Department of Pathology,** Institute for Developmental Research, Aichi Human Service Center, Kasugai, Japan*

**In mouse strains with the amyloidogenic apolipoprotein A-II (ApoA-II) gene (*Apoa2*$^c$), the type C ApoA-II protein (APOAIIC) associates to form amyloid fibrils AApoAII(C) that lead to development of early onset and systemic amyloidosis with characteristic heavy amyloid deposits in the liver and spleen. We found age-associated heavy deposition of amyloid fibrils [AApoAII(A)] composed of type A ApoA-II protein (APOAIIA) in BDF1 and C57BL/6 mice reared at one of our institutes. AApoAII(A) fibrils were deposited in the intestine, lungs, tongue, and stomach but not in the liver or spleen. AApoAII(A) fibrils were isolated, and morphological, biochemical, and structural characteristics distinct from those seen in AApoAII(C) and mouse AA amyloid fibrils were found. Transmission electron and atomic force microscopy showed that the majority of isolated AApoAII(A) amyloid fibrils featured fine, protofibril-like shapes. AApoAII(A) fibrils have a much weaker affinity for thioflavine T than for AApoAII(C), whereas APOAIIA protein contains less of the β-pleated sheet structure than does APOAIIC. The injection of AApoAII(A) fibrils induced amyloid deposition in C57BL/6 and DBA2 mice (*Apoa2*$^a$) as well as in R1.P1-*Apoa2*$^c$ mice (*Apoa2*$^c$), but AApoAII(A) induced more severe amyloidosis in *Apoa2*$^a$ strains than in the *Apoa2*$^c$ strain. It was found that AApoAII(A) fibrils isolated from mice with mildly amyloidogenic APOAIIA protein have distinct characteristics. Induction of amyloidosis by heterologous amyloid fibrils clearly showed interactions between amyloid protein monomers and fibrils having different primary structures.** ***(Am J Pathol 2004, 164:1597–1606)***

Amyloidosis is a structural disorder of proteins in which proteins that are normally soluble are deposited in tissues as abnormally ordered, insoluble amyloid fibrils made up of β-pleated sheets.[1] Several serious human diseases such as Alzheimer's disease, type II diabetes, prion diseases, and familial amyloid polyneuropathy are associated with amyloid fibril deposition.[2,3] Thus, to devise means of preventing amyloidosis, it may be essential to study the properties of amyloid proteins and the mechanisms for fibril formation. Many factors such as aging, the primary sequences and mutations of amyloid proteins, the genetic background of patients, and epigenetic factors, as well as the means of amyloid fibril transmission, may influence fibril formation.[4]

In mice, spontaneous senile amyloidosis has been found in many strains.[5] We isolated a unique amyloid fibril protein from the liver of the SAMP1 mouse strain and found that apolipoprotein A-II (ApoA-II), the second most abundant apoprotein of serum high-density lipoprotein, is deposited in the form of amyloid fibrils (AApoAII). These fibrils are deposited systemically, but not in the brain.[6,7]

Three alleles (*Apoa2*$^a$, *Apoa2*$^b$, and *Apoa2*$^c$) of the ApoA-II gene encode three variants of the ApoA-II protein (APOAIIA, APOAIIB, and APOAIIC) (Table 1).[8] Mice such as SAMP1, SAMP2, SAMP10, A/J, SJL/J, and SM/J, which have an APOAIIC protein with a glutamine at position 5, show a high incidence of severe senile amyloidosis, whereas the strains with a very low incidence of amyloidosis produce APOAIIB with a proline at position 5. Severe AApoAII amyloidosis is linked to the *Apoa2*$^c$ allele.[8–10] The C57BL/6, AKR/J, and DBA/2 strains encode an APOAIIA protein with Pro$^5$ and Met$^{26}$, and mild tissue-

Supported in part by the Ministry of Education, Culture, Sports, Science, and Technology of Japan [grants-in-aid for priority areas (15032217 and 15019036) and scientific research (B) (114380380)]; and the Ministry of Health, Labor, and Welfare of Japan.

Accepted for publication January 15, 2004.

Address reprint requests to Keiichi Higuchi, Department of Aging Biology, Institute on Aging and Adaptation, Shinshu University Graduate School of Medicine, Asahi 3-1-1, Matsumoto 390-8621, Japan. E-mail: khiguchi@sch.md.shinshu-u.ac.jp.

specific amyloidosis has been reported in these strains.[8] Aged C57BL/Ka mice were found to have a high incidence of gastrointestinal AApoAII amyloidosis.[11] AApoAII amyloidosis was observed in the ileum, lung, and heart of CD-1 Swiss mice,[12] and amyloid deposition was also seen in the renal glomeruli of NSY mice.[13] A better understanding of the mechanisms linking these unique tissue distribution patterns and the different degrees of deposition severity with the primary structures of ApoA-II proteins may shed light on amyloid fibrillogenesis.

Prion, an abnormal form ($PrP^{SC}$) of the host cellular prion protein ($PrP^{C}$), is responsible for transmissible spongiform encephalopathies (TSE), which include scrapie in sheep, bovine spongiform encephalopathy, and human Creutzfeldt-Jakob disease.[14,15] In TSE, the prion causes a conformational change of $PrP^{C}$ to $PrP^{Sc}$ and a detectable phenotype or disease in the affected individual. Recent studies with yeast have broadened the definition of prion from a proteinaceous infectious agent of TSE to a set of self-propagative proteins or protein-based genetic elements.[16] We described the prion-like transmission of AApoAII amyloidosis in reports of our previous studies. In the first of these, intravenous injection of AApoAII(C) fibrils markedly accelerated amyloid deposition in young R1.P1-*Apoa2*$^{C}$ mice.[17] In the second study, an *in vitro* experiment demonstrated that the extension of AApoAII(C) proceeds as a result of the linking of soluble APOAIIC to the ends of existing fibrils.[18] In the third study, we fed young R1.P1-*Apoa2*$^{C}$ mice with AApoAII(C) fibrils, or reared the young mice in the same cage with old R1.P1-*Apoa2*$^{C}$ mice that had severe amyloid deposits. All of these mice developed amyloid deposits.[19] Lastly, we found that AApoAII(C) induced a conformational change in the less-amyloidogenic APOAIIB to a different amyloid fibril structure, and that this protein could also induce amyloidosis in the less-amyloidogenic SAMR1 strain.[20]

In the study presented here we detected early onset and heavy AApoAII(A) amyloid deposition in BDF1 and C57BL/6 mice, and were able to isolate enough amyloid fibrils for biochemical and morphological characterization, as well as for studies on transmission of amyloidosis. The AApoAII(A) fibrils proved to have unique features and provided new insights into the process of amyloidogenesis.

## Materials and Methods

### Animals

BDF1 are hybrid mice obtained by breeding female C57BL/6CrSlc (C57BL/6) mice with male DBA/2CrSlc (DBA/2) mice. BDF1 and C57BL/6 mice were purchased from Japan SLC, Inc. (Hamamatsu, Japan) and kept at the Tokyo Metropolitan Institute of Gerontology. They were raised under specific pathogen-free conditions at 24°C with a light-controlled regimen (12 hours light/dark cycle). A commercial diet (CRF-1; Oriental Yeast Co., Ltd., Tokyo, Japan) and sterile water were available *ad libitum*. BDF1 mice at the ages of 4, 9, 14, 19, 25, and 31 months and C57BL/6 mice at 12 and 24 months of age were killed by cardiac puncture under diethyl ether anesthesia. Tissues from the whole body were fixed in 10% neutral buffered formalin, embedded in paraffin, and cut into 4-$\mu$m sections for hematoxylin and eosin, Congo-red, and immunohistochemical staining.[7] The intestines and livers were stored at −70°C for biochemical analysis. Animal studies were conducted in accordance with guidelines for the use of laboratory animals of the Tokyo Metropolitan Institute of Gerontology.

### Induction of Amyloidosis by Injection of AApoAII Amyloid Fibrils

AApoAII amyloidosis was induced in 2-month-old female R1.P1-*Apoa2*$^{c}$, C57BL/6, DBA/2, and B6RCF1 mice by injection of amyloid fibrils (Table 1). A congenic strain, R1.P1-*Apoa2*$^{c}$, features the amyloidogenic ApoA-II gene (*Apoa2*$^{c}$) of the SAMP1 strain on the genetic background of the less-amyloidogenic SAMR1 strain.[21] R1.P1-*Apoa2*$^{c}$ mice were maintained through sister-brother mating at the Division of Laboratory Animal Research, Research Center for Human and Environmental Science, Shinshu University. F1 hybrid mice B6RCF1 were obtained by breeding female C57BL/6 mice with male R1.P1-*Apoa2*$^{c}$ mice. AApoAII(A) amyloid fibrils were isolated from the BDF1 intestines and AApoAII(C) fibrils were obtained from the livers of aged R1.P1-*Apoa2*$^{c}$ mice. These fibrils were then suspended in pure water and samples (0.1 mg), prepared freshly without freezing, were injected intravenously after sonication.[17] Mice strains and injected amyloid fibrils used in this study are summarized in Table 1. The mice were reared under specific pathogen-free conditions at 24°C with a light controlled regimen (12 hours light/dark cycle). A commercial diet (MF; Oriental Yeast, Co., Ltd.) and tap water were available *ad libitum*. Animal studies were conducted in accordance with the guidelines for the use of laboratory animals of Shinshu University School of Medicine. Three and 6 months after injection of amyloid fibrils, the mice were killed as described above.

### Detection of Amyloid Deposition

Depositions of amyloid fibrils were identified by their green birefringence in Congo Red-stained sections, vis-

**Table 1.** Mice Strains and Amyloid Proteins Used in this Investigation

| Mouse strain | ApoA-II allele | ApoA-II protein | Amino acid substitution | Amyloid fibrils | Amyloidosis |
|---|---|---|---|---|---|
| BDF1, C57BL/6J, DBA/2 | *Apoa2*$^{a}$ | APOAIIA | 5Pro,26Val,38Val | AApoAII(A) | Mild |
| R1.P1-*ApoA2*$^{c}$, SAMP1 | *Apoa2*$^{c}$ | APOAIIC | 5Gln,26Ala,38Met | AApoAII(C) | Severe |
| B6RCF1 | *Apoa2*$^{a/c}$ | APOAIIA/APOAIIC | | AApoAII(A) | |

ible with polarizing microscopy. The amyloid fibril proteins, AApoAII and AA, were identified immunohistochemically with the avidin-biotinylated horseradish peroxidase complex method using specific antiserum against murine AApoAII and AA.[7] SAP and ApoE were also identified immunohistochemically using specific antiserum against murine SAP (Calbiochem-Novabiochem Co., San Diego, CA) and ApoE (CorTex Biochem, Inc., San Leandro, CA). The intensities of the AApoAII amyloid depositions were determined semiquantitatively according to the amyloid index (AI). The AI represented the mean value of the amyloid deposition scores, graded from 0 to 4, for the seven major tissues (liver, spleen, tongue, heart, intestine, stomach, and skin) that were stained with Congo Red, as described previously.[19,20] Tissues were examined by two independent observers who were blinded to the experimental protocol.

The method for *in situ* electron microscopic observations of amyloid fibrils has been described previously.[22] Small blocks (1 $mm^3$) of the intestine and tongue from aged BDF1 mice (29 months) were fixed with 3% glutaraldehyde in 0.1 mol/L sodium cacodylate (pH 7.4) for 3 hours at room temperature and postfixed with osmium tetraoxide in the same buffer for 1.5 hours at 4°C. *En block* staining was performed with 1.0% uranyl acetate in 70% ethanol for 40 minutes at 4°C. Thin sections of tissues embedded in Epon were placed on a copper grid and examined at an accelerating voltage of 70 kV under a Hitachi H-7000 electron microscope (Hitachi Ltd., Tokyo, Japan).

### *Isolation of Amyloid Fibrils*

The amyloid fibril fraction was isolated as a suspension in water from the livers and intestines of 20-month-old R1.P1-*Apoa2*$^c$ mice and from the intestine, lungs, tongue, and stomach of 31-month-old BDF1 mice.[19] These fibrils were then used for biochemical and morphological analyses. AA fibrils were extracted from the livers of 24-month-old C57BL/6 mice with severe inflammation.

Tris-Tricine/sodium dodecyl sulfate-polyacrylamide gel electrophoresis was performed on 16.5% acrylamide gels.[23] Proteins were visualized by means of Coomassie Brilliant Blue R250. The duplicated part of the gel was transferred electrophoretically to a polyvinylidene difluoride membrane (Bio-Rad Laboratories, Hercules, CA). Proteins that reacted with anti-AApoAII and anti-AA antibody were visualized by using biotinylated pig anti-rabbit immunoglobulin, avidin combined with horseradish peroxidase, and 3, 3′-diaminobenzidine.[24]

### *Transmission Electron Microscopy (TEM) and Atomic Force Microscopy (AFM) Imaging of Amyloid Fibrils*

A suspension of AApoAII(A), AApoAII(C), and AA amyloid fibrils (0.1 to 1.0 mg/ml) in 5 $\mu$l of water, stained negatively with 5 $\mu$l of 2% sodium phosphotungstate (pH 7.2), was spread on a carbon-stabilized Formvar-membrane (Okenshoji Co., Ltd., Tokyo, Japan).[25] These samples were then examined under a JEM1200 transmission electron microscope (JEOL Ltd., Tokyo, Japan) with acceleration at 80 kV. For AFM observations an SPI-3800N with DF40 cantilevers (Seiko Instruments, Chiba, Japan) and a spring constant of 40 N/m was used. The 5-$\mu$l water suspensions of amyloid fibrils (0.3 mg/ml) were spread on the surface of freshly cleaved mica and excess water was removed with a gentle stream of air.

### *Biochemical Characterization of Amyloid Fibrils*

An RF-1500 spectrofluorometer (Shimazu Corp., Kyoto, Japan) was used for fluorescence spectroscopy at room temperature. In all experiments, the size of the reaction mixture was 1.0 ml and the reactions were performed in polypropylene tubes (1.5 ml) at room temperature. The incubation mixture contained 50 mmol/L glycine-NaOH buffer (pH 9.0), 5 $\mu$g of amyloid fibrils, and various concentrations of thioflavine T (ThT) (Wako Pure Chemical Industries, Ltd., Osaka, Japan). Five-$\mu$l aliquots from each of the reaction tubes were used for fluorescence spectroscopy. In all studies, emission spectra at 482 nm were obtained.[25]

Both APOAIIA and APOAIIC monomers were obtained from amyloid fibrils by means of six molar urea polyacrylamide gel electrophoreses.[18] Each type of monomer (20 $\mu$g) was dissolved in phosphate buffer (50 mmol/L, pH 7.5). The circular dichroism (CD) spectrum of each protein solution was recorded on a Jasco 725 spectrometer (JASCO Corp., Tokyo, Japan) at 25°C, and at 0.2-nm intervals between wavelengths of 194 and 250 nm.

### In Vitro *Polymerization Assay*

Reaction mixtures (40 $\mu$l) contained 25 mmol/L phosphate buffer at pH 7.5, 100 $\mu$mol/L (35 $\mu$g) APOAIIA or APOAIIC monomer purified from high-density lipoprotein of C57BL/6 and R1.P1-*Apoa2*$^c$ mice,[5] 3 $\mu$g of sonicated AApoAII(A) or AApoAII(C) fibrils, and 300 $\mu$mol/L urea. For the inhibition analysis, various amounts of APOAIIA monomers were added to the reaction mixtures, which were prepared at 4°C. Reactions were performed in tubes at 37°C three times. Five-$\mu$l aliquots from each reaction tube were used for fluorescence spectroscopy.[25]

### *Statistical Analysis*

Significant differences in the values of AIs among the various groups of mice were examined using the Mann-Whitney *U*-test.

## *Results*

### *Amyloid Deposition in BDF1 and C57BL/6 Mice*

Sequence analysis of ApoA-II cDNA revealed that both BDF1 and C57BL/6 have the *Apoa2*$^a$ allele of the ApoA-II gene (data not shown). The intensity of amyloid deposi-

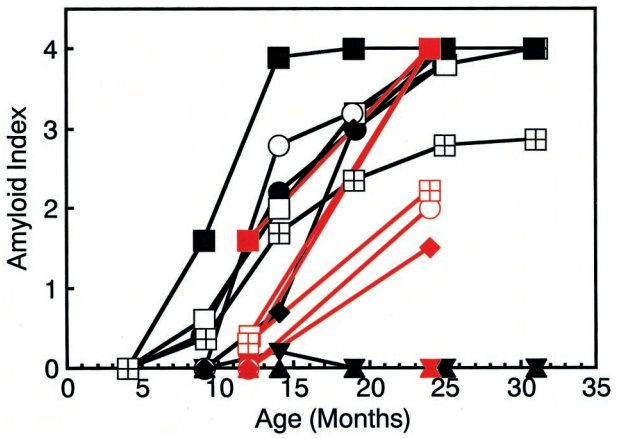


**Figure 1.** Age-associated increase in amyloid deposition in BDF1 mice. Five mice in each age group were examined. AI determined by Congo Red staining in the tongue (■), heart (○), stomach (●), intestine (□), skin (♦), liver (▼), spleen (▲), and whole body (⊞) were plotted against age. **Black symbol**, BDF1; **red symbol**, C57BL/6.

tion in BDF1 mice increased with age (Figure 1), while no amyloid deposits were seen in young mice (4 months of age), and only slight depositions in the tongue, intestine, and stomach were seen in mice at the age of 9 months. In the aged mice (25- and 31-month-old), however, the grade of amyloid deposition in the intestine, tongue, stomach, skin, and heart was nearly 4, which means corresponding to severe and systemic deposition, although no deposits were observed in the livers and spleens of these mice.

The amyloid deposit stained positively with anti-AApoAII antiserum and negatively with the anti-AA antiserum (Figure 2; A to C). The villi in the intestines of aged BDF1 mice were filled with amyloid deposits, whereas other tissues such as tongue, heart, and stomach also contained severe AApoAII deposition (Figure 2; D to F). The amyloid deposit in the villi and other tissues of aged BDF1 stained positively with antiserum against mouse SAP and ApoE (Figure 2; G to I). *In situ* TEM showed amyloid fibril-like components ~8 nm wide in the intestines and tongues of aged BDF1 mice (Figure 3).

The degrees of amyloid deposition in the C57BL/6 mice at the ages of 12 and 24 months are summarized in Figure 1. Aged C57BL/6 (24 months) mice also showed severe amyloid deposition in the intestine, stomach, and tongue. In two 24-month-old C57BL/6 mice, AA fibrils were deposited in the spleen and liver (data not shown). AA fibrils were extracted from all of these tissues.

## *Isolation of Amyloid Fibrils*

Amyloid fibril fractions were extracted from various tissues of aged BDF1 and R1.P1-*Apoa2*$^{c}$ mice and analyzed by sodium dodecyl sulfate-polyacrylamide gel electrophoresis. A dominant single band having a molecular weight of ~8.6 kd was detected (Figure 4A), which was consistent with the size of the ApoA-II monomer. Additional bands in the molecular weight range 10 ~ 18 kd were observed in the lung fraction. Western blotting of the amyloid fibril fractions extracted from the intestines of the BDF1 mice with anti-AApoAII or anti-mouse AA antibody produced two bands reacting with the anti-AApoAII antibody (Figure 4B). The same results were obtained for the amyloid fractions from the other tissues (data not shown). These bands indicated the presence of the ApoA-II monomer (molecular weight, ~8.6 kd) and dimer (molecular weight, ~18 kd). No specific band was stained with the anti-mouse AA antibody. The amyloid fraction from the intestine of the BDF1 mice was not stained with anti-ApoE or anti-transthyretin antiserum (Santa Cruz Biotechnology, Inc., Santa Cruz, CA) (data not shown).

## *Morphological Characterization of Amyloid Fibrils*

TEM images of AApoAII(C) fibrils showed the typical helical structure of amyloid fibrils (Figure 5A), which were 10 nm in diameter, rigid, and nonbranching. Mouse AA also showed typical amyloid fibrils that were nonbranched, 8-nm-wide fibril structures (Figure 5B). On the other hand, typical fibril images were rarely obtained in the case of AApoAII(A) fibrils, but fibrils with a spherical shape (Figure 5C) and short fibril-like materials with a width of ~5 nm were observed (Figure 5D). AFM images of amyloid fibrils showed typical amyloid fibrils of AApoAII(C) (height up to 10 nm) and mouse AA (height up to 8 nm) (Figure 5, E and F), whereas fine and small fibrils (height up to 2 nm) and very small amounts of larger and longer fibrils (height up to 7 nm) were found in the amyloid fibril fractions from BDF1 mice (Figure 5, G and H).

## *Affinity of Amyloid Fibrils for ThT*

Morphological differences observed among AApoAII(A), AApoAII(C), and AA fibrils suggested that the biochemical properties of these amyloid fibrils may be different. ThT binds to amyloid fibrils and emits fluorescence at a specific wavelength. The binding constant Kb was defined as the concentration of ThT that produced half of the maximum emission intensity at 482 nm. AApoAII(C) from the R1.P1-*Apoa2*$^{c}$ liver indicated a strong affinity for ThT (kb = 106 nmol/L) (Figure 6), as did AApoAII(C) from the R1.P1-*Apoa2*$^{c}$ intestine (kb = 35 nmol/L). On the other hand, AApoAII(A) from the BDF1 intestine showed a much weaker affinity (kb = 4.2 $\mu$mol/L). AA fibrils were characterized by a typical amyloid fibril structure, but the affinity was much weaker (kb = 5.6 $\mu$mol/L) than that of AApoAII(C). The affinity of Congo Red for AApoAII(A) fibrils *in vitro* was weaker than that for AApoAII(C) fibrils (data not shown).

## *CD Analysis of Secondary Structure of ApoA-II*

To evaluate the conformational differences between the two types of ApoA-II monomers, a CD analysis was performed using ApoA-II monomers at neutral pH. These monomers had been used for polymerization reactions of

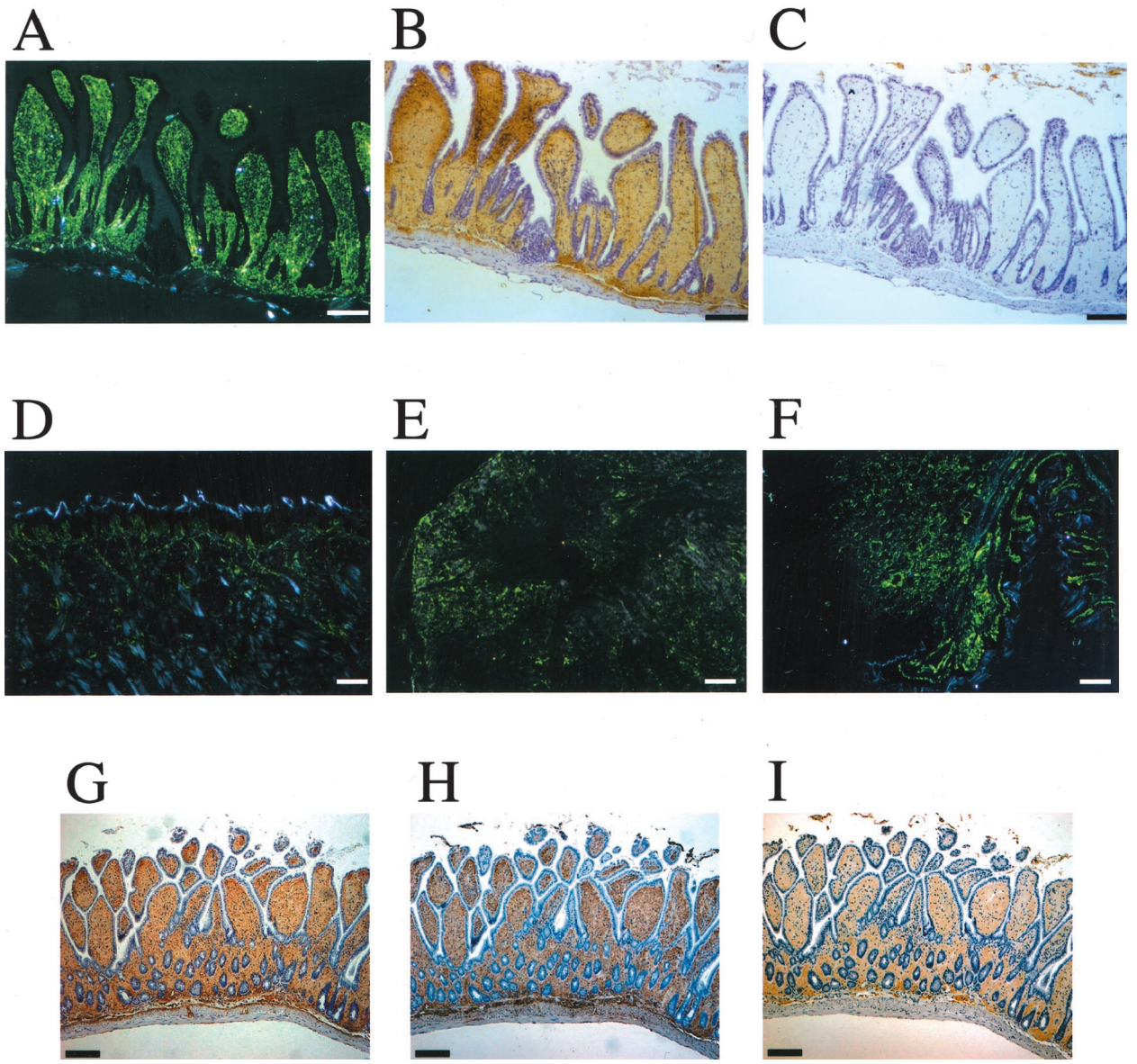


**Figure 2.** AApoAII deposition in tissues of aged BDF1 mice. Amyloid deposition in an aged (31 months) BDF1 mouse was detected by green birefringence in Congo Red-stained sections examined by polarized microscopy (**A**, **D**, **E**, and **F**). Amyloid proteins were identified immunohistochemically with anti-AApoAII (**B**) and anti-AA antiserum (**C**). **A:** Amyloid deposit (grade 4) in the intestine. **B:** AApoAII deposits identified in the intestine by staining with anti-AApoAII antiserum. **C:** No AA was detected in the intestine by staining with anti-AA antiserum. Amyloid deposition represented by green birefringence in the tongue (grade 4) (**D**), stomach (grade 4) (**E**), and heart (grade 4) (**F**). **G:** AApoAII deposits identified in the intestine by staining with anti-AApoAII antiserum. **H:** SAP was identified in the intestine by immunohistochemical staining. **I:** ApoE was identified in the intestine by immunohistochemical staining. Scale bars, 100 $\mu$m.

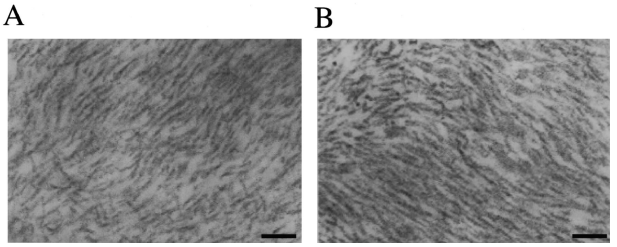


**Figure 3.** *In situ* TEM of amyloid deposition in aged BDF1 mice. AApoAII(A) amyloid fibrils were detected in the intestine (**A**) and tongue (**B**) of an aged (29 months) BDF1 mouse. Gently curved, ~8-nm-wide entities were observed. Scale bar, 100 nm.

amyloid fibrils *in vitro* (Figure 7). In the case of the APOAIIA monomer, the spectrum exhibited only a negative ellipticity with a negative peak at 201 nm. This indicates that this protein has a nonhelical, non-$\beta$-strand secondary structure. On the other hand, the spectrum of APOAIIC exhibited a trough at a higher wavelength, demonstrating that APOAIIC has a more extensive $\beta$-sheet structure than does APOAIIA.

## In Vitro *Fibril Formation by Type A ApoA-II*

To examine fibril formation *in vitro*, AApoAII(C) and AApoAII(A) fibrils and 100 $\mu$mol/L of two types of ApoA-II monomers were incubated at 37°C in phosphate buffer

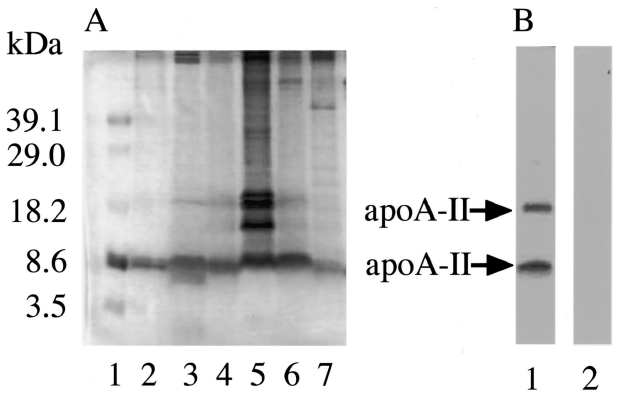


**Figure 4.** AApoAII(A) amyloid fibril deposits in various mouse tissues of aged BDF1 mice. Amyloid fibrils were extracted as water-suspended fractions and were separated by sodium dodecyl sulfate-polyacrylamide gel electrophoresis. **A:** The gel was stained with Coomassie Brilliant Blue R-250. Molecular weight marker (**lane 1**), AApoAII(C) amyloid fibrils of the liver (**lane 2**) and the intestine (**lane 3**) of R1.P1-*Apoa2*$^{C}$ mice. AApoAII(A) amyloid fibrils of the intestine (**lane 4**), lungs (**lane 5**), stomach (**lane 6**), and tongue (**lane 7**) of aged BDF1 mice. **B:** Western blot analysis of AApoAII(A) amyloid fibrils from the intestine of a BDF1 mouse, detected with anti-AApoAII antiserum (**lane 1**) and anti-AA antiserum (**lane 2**).

(pH 7.5). AApoAII(C) fibrils act as seeds for AAPOAIIC monomers, resulting in extension of the amyloid fibrils (Figure 8A). However, fibril extension *in vitro* was not detected in the reaction of APOAIIA monomer with

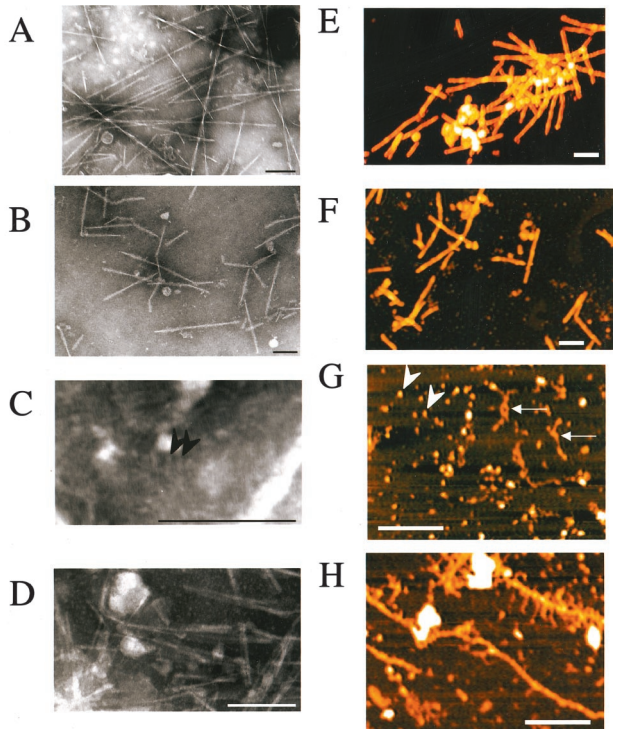


**Figure 5.** TEM and AFM images of amyloid fibrils. AApoAII(C) amyloid fibrils from the liver of R1.P1-*Apoa2*$^{C}$ (**A**), and AA fibrils from the spleen of C57BL/6 mice (**B**) were negatively stained. These amyloid fibrils were rigid, nonbranching, and 8 to 10 nm wide. AApoAII(A) amyloid fibril fractions contained fine or spherical (2 nm wide, **arrowheads**) (**C**), or thin (5 nm wide), short fibril-like materials (**D**). AFM images of amyloid fibrils show typical amyloid fibrils of AApoAII(C) (height up to 10 nm) (**E**), and mouse AA (height up to 8 nm) (**F**). Spherical-shaped fibrils (**arrowheads**) and fine fibrils (height up to 2 nm, **arrows**) (**G**), and a very small amount of larger and longer fibrils (height up to 7 nm) (**H**) were found in amyloid fibril fractions from the intestines of BDF1 mice. Scale bar, 200 nm.

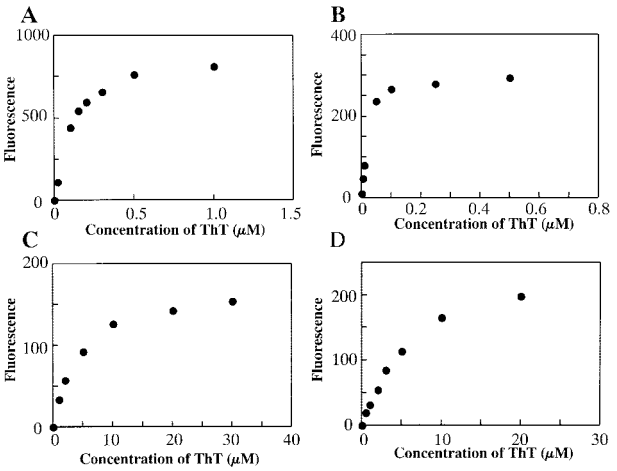


**Figure 6.** The affinity of amyloid fibrils for ThT. The effects of various ThT concentrations on the fluorescence of amyloid fibrils were determined. **A:** AApoAII(C) isolated from the liver; **B:** AApoAII(C) isolated from the intestine; **C:** AApoAII(A); and **D:** mouse AA. AApoAII(C) fibrils were isolated from the liver and intestine of a 19-month-old R1.P1-*Apoa2*$^{C}$ mouse. Mouse AA fibrils were isolated from the liver of a 24-month-old C57BL/6 mouse. AApoAII(A) fibrils were isolated from the intestine of a 31-month-old BDF1 mouse. AApoAII(C) fibrils showed a strong affinity for ThT (106 nmol/L or 35 nmol/L). On the other hand, AApoAII(A) and mouse AA showed relatively weak affinities (4.2 $\mu$mol/L and 5.6 $\mu$mol/L, respectively). Similar results were observed in three independent experiments, and typical data are shown.

AApoAII(A) fibrils (data not shown). Fibril extension of AApoAII(C) in reaction with APOAIIC was inhibited by the APOAIIA monomer. AApoAII(C) fibrils and 100 $\mu$mol/L APOAIIC monomer were incubated with various concentrations of the APOAIIA monomer. Fibril formation was significantly reduced with an increase in APOAIIA monomer concentration (Figure 8B). Equivalent amounts of APOAIIA (100 $\mu$mol/L) inhibited fibril formation by 80%.

## *Induction of Amyloidosis* in Vivo

Sonicated AApoAII(A) or AApoAII(C) amyloid fibrils (100 $\mu$g) were injected intravenously into 2-month-old R1.P1-

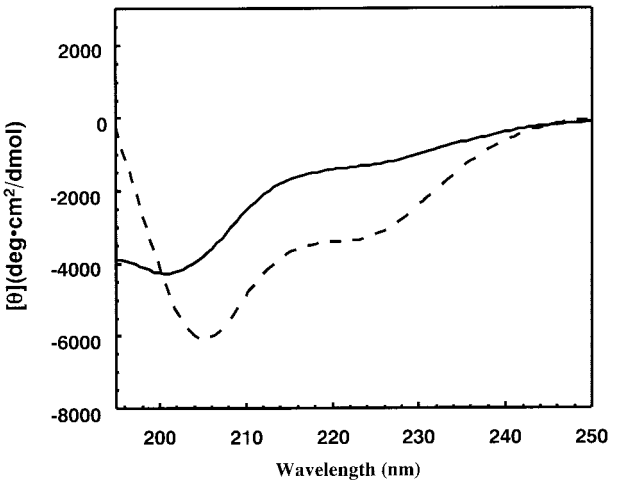


**Figure 7.** CD spectra of APOAIIA and APOAIIC amyloid precursor proteins. APOAIIA protein (**solid line**) and APOAIIC protein (**broken line**) were isolated from AApoAII(A) and AApoAII(C) amyloid fibrils, respectively. Each protein was dissolved in neutral phosphate buffer (pH 7.5).

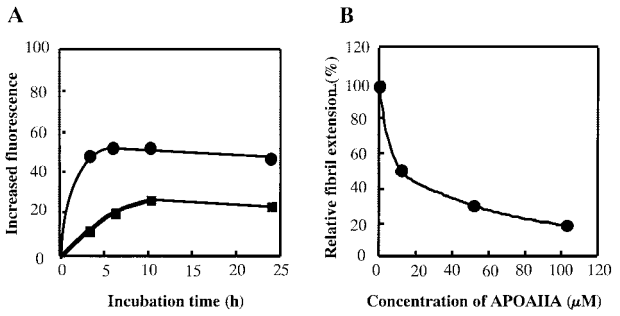


**Figure 8.** *In vitro* fibril extension kinetics of the APOAIIA amyloid protein. **A:** Samples (100 μmol/L) of APOAIIC proteins were incubated with 75 ng/μl of AApoAII(C) seeds in 25 mmol/L phosphate buffer, pH 7.5, and 300 mmol/L urea without (●) or with 70 μmol/L APOAIIA proteins (■) at 37°C for 0, 3, 7, 10, and 24 hours. **B:** APOAIIC proteins (100 μmol/L) were incubated with 75 ng/μl AApoAII(C) seeds and with various amounts (0, 10, 50, and 100 μmol/L) of APOAIIA proteins at 37°C for 10 hours. Inhibition of fibril extension by APOAIIA proteins was determined. Similar results were observed in three independent experiments, and typical data are shown.

*Apoa2*$^c$, C57BL/6, DBA/2, and B6RCF1 mice (Table 2). Three months after injection of AApoAII(C) into R1.P1-*Apoa2*$^c$ mice, amyloid deposition was detected in all of the organs examined (AI = 2.4). Six months after injection of AApoAII(C), amyloid deposition had increased (AI = 3.3). Severe deposition was detected in the tongue, the Disse's space of the periportal sinusoid of the liver, spleen, stomach, interstitia of heart muscles, and intestine. When AApoAII(C) fibrils were injected into mice, R1.P1-*Apoa2*$^c$ had the most severe amyloidosis seen among four strains. AApoAII(A) also induced amyloidosis in R1.P1-*Apoa2*$^c$ mice, but the intensity of amyloidosis was weaker than that induced by AApoAII(C) (AI = 1.3, $P = 0.0003$ at 3 months).

C57BL/6 and DBA/2 mice, which have the APOAIIA proteins, showed mild or slight amyloid deposition after injection of AApoAII(C) fibrils. Three months after injection, deposition was found in the intestine, tongue, and stomach, but no deposition was seen in the liver or spleen (AI = 0.5). Six months after injection, the degree of amyloidosis had also increased, and amyloid deposition was detected in the liver and spleen of C57BL/6 mice (AI = 1.9). Amyloidosis in these mice was induced by injection of AApoAII(A). Three months after injection, amyloid deposition was detected in the tongue, stomach, interstitia of heart muscles, and intestine (AI = 1.1, C57BL/6). After 6 months, the deposition in these tissues had become more severe (AI = 2.3), but no amyloid deposition was shown in the liver or spleen. The degree of induction by AApoAII(A) was stronger than that by AApoAII(C) in both of the *Apoa2*$^a$ strains ($P < 0.01$).

Only slight amyloid deposition in the intestine was induced by AApoAII(C) fibrils in B6RCF1 mice, which possess both APOAIIA and APOAIIC proteins. AApoAII(A) fibrils also induced amyloidosis in the B6R1CF1 mice. The intensity of deposition by AApoAII(A) fibrils was much stronger than that induced by AApoAII(C) ($P = 0.0002$ at 3 months). AApoAII fibrils deposited in the tongue of the B6R1CF1 mice injected with APOAIIA were proven to be AApoAII(A) by mass spectrometry, and these had a molecular weight of 8709 (data not shown). No amyloid deposition was detected in water-injected control mice of any strains used for these experiments.

## Discussion

Amyloidosis, in which proteins associate to form abnormally ordered, fibril-like structures, is a complex pathological condition. Both genetic and epigenetic factors contribute to the initiation and progression of this disease set. Mouse AApoAII amyloidosis can be studied to unravel the complex pathogenesis of this condition. Three alleles of the mouse *Apoa2* gene have been reported.[5] Amyloidosis whose intensity and tissue distribution depends on the mouse strain and on the specific rearing conditions has been reported in the *Apoa2*$^a$ strains.[11–13] In this study, we found that AApoAII(A) amyloid fibrils isolated from mild-amyloidogenic BDF1 mice have distinct pathological and structural characteristics and transmissibility patterns.

Severe systemic amyloidosis is seen in the *Apoa2*$^c$ strains, but little or none is seen in the *Apoa2*$^b$ strains. APOAIIA and APOAIIB proteins contain a proline at position 5, while the APOAIIC protein has a glutamine at position 5. Proline is known to break up β-sheets,[26] while

**Table 2.** Induction of Amyloidosis by the Injection of Two Kinds of AApoAII Amyloid Fibrils in Various Strains of Mice

| Strain | *Apoa2* | Injected amyloid fibrils | Number of mice | AI* (3M)T | | | | | | | | Number of mice | AI (6M)T | | | | | | | |
|---|---|---|---|---|---|---|---|---|---|---|---|---|---|---|---|---|---|---|---|---|
| | | | | Liv | Spl | Int | Stm | on | Her | Skn | Total | | Liv | Spl | Int | Stm | on | Her | Skn | Total |
| R1.P1-*Apoa2*$^C$ | c/c | AApoAII(C) | 14 | 2.1 | 2.5 | 2.5 | 2.2 | 3.4 | 2.1 | 1.9 | 2.4$^b$ | 9 | 3.4 | 3.8 | 3.6 | 3.8 | 3.3 | 3.1 | 2.2 | 3.3$^h$ |
| | | AApoAII(A) | 7 | 0.0 | 0.1 | 2.4 | 2.1 | 2.5 | 1.0 | 0.7 | 1.3$^a$ | 7 | 2.0 | 2.2 | 2.0 | 3.0 | 3.9 | 2.1 | 2.4 | 2.5$^g$ |
| C57BL/6 | a/a | AApoAII(C) | 6 | 0.0 | 0.0 | 0.3 | 1.2 | 2.0 | 0.0 | 0.2 | 0.5$^d$ | 5 | 2.0 | 0.2 | 2.7 | 2.9 | 2.9 | 0.9 | 1.4 | 1.9$^j$ |
| | | AApoAII(A) | 7 | 0.0 | 0.0 | 0.8 | 2.1 | 2.9 | 1.1 | 1.1 | 1.1$^c$ | 7 | 0.4 | 0.0 | 2.6 | 3.1 | 3.9 | 3.7 | 2.3 | 2.3$^i$ |
| DBA/2 | a/a | AApoAII(C) | 7 | 0.6 | 0.0 | 1.2 | 1.0 | 1.7 | 0.2 | 0.0 | 0.7 | 5 | 2.9 | 0.0 | 2.7 | 1.6 | 2.4 | 1.1 | 0.0 | 1.5$^l$ |
| | | AApoAII(A) | 6 | 0.0 | 0.0 | 1.3 | 1.4 | 1.8 | 1.2 | 0.2 | 0.8 | 6 | 0.0 | 0.0 | 3.9 | 2.5 | 3.5 | 3.6 | 0.8 | 2.1$^k$ |
| B6RCF1 | a/c | AApoAII(C) | 9 | 0.0 | 0.0 | 0.5 | 0.0 | 0.1 | 0.0 | 0.1 | 0.1$^f$ | 7 | 0.0 | 0.0 | 0.4 | 0.5 | 0.6 | 0.1 | 0.0 | 0.2$^n$ |
| | | AApoAII(A) | 10 | 0.0 | 0.0 | 0.3 | 2.2 | 3.2 | 0.2 | 0.5 | 1.0$^e$ | 5 | 0.0 | 0.9 | 1.7 | 2.8 | 3.5 | 1.8 | 1.8 | 1.8$^m$ |

No amyloid deposition was detected in water-injected control mice of each strain at 3 months and 6 months after injection (data are from ~ five mice).

*The AI was determined after 3 and 6 months for each mouse injected with amyloid fibrils and the mean AI values are shown. Liv, liver; Spl, spleen; Int, intestine; Stm, stomach; Ton, tongue; Her, heart; and Skn, skin.

The AI of whole body (total AI) of different groups of mice was compared using the nonparametric Mann-Whitney *U*-test. Within one column, values with different letters (a *versus* b, c *versus* d, e *versus* f, g *versus* h, i *versus* j, k *versus* l, and m *versus* n) are significantly different ($P < 0.05$).

glutamine is able to generate polar interactions that stabilize the β-sheet conformation,[27] and is therefore postulated to be fibrillogenetic. In addition, APOAIIA features a Val26Met substitution from the less-amyloidogenic APOAIIB protein. Amyloidogenic mutations from valine to methionine have been identified in familial amyloid polyneuropathy.[28,29] We found a characteristic tissue distribution of amyloid deposition in BDF1 and C57BL/6 mice, which showed severe depositions in the intestine and tongue but no depositions in the liver and spleen, where major amyloid deposits were observed in the *Apoa2*$^{c}$ strains. Similar observations have been reported for human hereditary amyloidosis. In the first, the apolipoprotein A-I (ApoA-I) variant Gly26Arg was found to be associated with peripheral neuropathy, peptic ulcers, and nephrotic syndrome.[30] In another study, a deletion/insertion mutation in exon 4 of the ApoA-I gene proved to be capable of causing amyloid hepatopathy,[31] and variant Leu90Pro mutants of ApoA-I are associated with cutaneous amyloid deposition and cardiomyopathy.[32] It has been suggested that this phenomenon is related to the distinct primary structure and conformation of the amyloid fibrils.[33] However, the Leu55Pro mutant of TTR is known to be amyloidogenic,[34] and the Val30Met mutant has a variety of tissue phenotypes.[35] Thus, it may be difficult to be evaluate the possible role of each amino acid substitution in amyloid deposition.

Isolated AApoAII(A) fibrils have a conformation distinct from that of amyloidogenic AApoAII(C) in that they have: 1) a proto-fibril-like structure; 2), less affinity for ThT; 3) a smaller amount of β-pleated sheet structure in the monomer form. TEM and AFM detected very fine (~2 nm) proto-fibril-like structures and extremely few fibrils, and these were shorter and thinner than the AApoAII(C) and AA fibrils. The presence of protofibril-like fibrils has been reported in immunoglobulin light-chain,[36] Aβ,[37] and other types of amyloid proteins such as TTR, in *in vitro* fibril formation.[38] Depositions of nonfibrillar amyloid protein have been reported in light chain deposition disease,[39] in a Val30Met familial amyloid polyneuropathy patient[40] and in Leu55Pro[41] and normal TTR transgenic mice.[42] Tissue sections from BDF1 mice that were stained with Congo Red showed a distinct apple-green birefringence, and *in situ* electron microscopy disclosed mature fibril-like components. In addition, amyloid deposits in BDF1 were found to have SAP and ApoE. These phenomena suggest the presence of the fibrillar form *in situ*. In the case of BDF1 mice, the amount of amyloid fibrils may be small, so only small amount of fibrils can be detected with TEM and AFM. The significance of the reduced affinity of AApoAII(A) amyloid fibrils for ThT remains to be explained. However, because ThT recognizes the amyloid fibril structure, minor conformational variations may give rise to differences in the affinity for ThT.[25] We found by CD that the APOAIIA protein contains fewer β-pleated sheets and random structures at neutral pH than does APOAIIC. These results indicate that specific structural and morphological features of the amyloid protein may explain the different degrees of deposition severity and the unique tissue distribution of amyloids. However, the precise mechanism of this relationship awaits further clarification.

Recent research has suggested that amyloid fibrils, like prions, are self-propagating protein conformations occurring both *in vitro* and *in vivo*.[18,43–45] When small nuclei or amyloid fibrils are present, they dramatically accelerate fibril formation by inducing conformational changes in amyloid protein monomers, which adopt the same fibrillar structure as amyloid fibrils. Both AApoAII(C) and AApoAII(A) fibrils were found to be capable of inducing amyloidosis. The relative intensities of induction by homologous amyloid fibrils [R1.P1-*Apoa2*$^{c}$ by AApoAII(C) and BDF1, C57BL/6 by AApoAII(A)] were greater than the induction intensities in the heterogeneous amyloid fibrils [R1.P1-*Apoa2*$^{c}$ by AApoAII(A) and the *Apoa2*$^{a}$ strains by AApoAII(C)]. AApoAII(A) fibrils induced both types of AApoAII amyloidosis with the same intensity, but AApoAII(C) fibrils induced AApoAII(C) amyloidosis much more strongly. In B6RCF1mice that coexpress both APOAIIA and APOAIIC, induction of amyloidosis by AApoAII(C) was remarkably suppressed. This result agreed with the *in vivo* observations that F2 hybrid mice with the *Apo2*$^{a/c}$ allele showed no amyloid deposition[8] and that AAPOAIIA monomer inhibited fibrillar extension of APOAIIC that was seeded with AApoAII(C) *in vitro* (Figure 8). On the other hand, an appreciable amount of AApoAII(A) was deposited in B6RCF1 mice when AApoAII(A) was injected. The tissue distribution of amyloid deposits was related to the type of endogenous ApoA-II protein and did not depend on the type of injected amyloid fibrils. AApoAII(A) amyloid fibrils were not detected in the spleen and liver in BDF1, C57BL/6, and B6RCF1 mice injected with AApoAII(C) (Table 2).

Amyloidosis, including prion diseases, results from a conformational change in a protein, and this conversion makes the disease transmissible.[4,19,43,44,46] Transmission of exogenous amyloid fibrils can be an epigenetic initiator of amyloidosis under certain conditions. Previous studies have indicated the existence of a species barrier in mammalian and yeast prions, which depends on differences in primary structures among prion proteins.[47,48] However, recent research has demonstrated that the appearance of yeast prions is enhanced by heterologous prion aggregates.[49] Acceleration of amyloidosis by heterologous amyloid fibrils was detected in AA and AApoAII amyloidosis.[20,50] It has also been proposed that the seeding model can be used to explain how injected amyloid fibrils, synthetic amyloid-like fibrils or modified silk enhances the elongation of amyloid fibrils in mice.[51,52] More than 30 amyloid proteins and fibrils have been identified in humans and mice,[4] and recent investigations have reported the presence of amyloid fibrils in fungus and in *Escherichia coli*.[53,54] Computer searches revealed that 108 of the ~6000 *Saccharomyces cerevisiae* genes contain prion-like domains.[55] If enhancement of amyloid fibril formation by other amyloid fibrils is a widespread phenomenon, it may be one of general pathogenesis common to various kinds of amyloidosis.

We first isolated and characterized a mildly amyloidogenic variant of mouse AApoAII amyloid fibrils [AApoAII(A)] from the commonly used BDF1 and C57BL/6 mice. AApoAII(A) has unique structural properties. The intensity of AApoAII(A) deposition is highly de-

pendent on the conditions under which the mice are reared, because we could not find any amyloid deposition in the C57BL/6 and BDF1 mice in other laboratories (data not shown). Thus, multiple factors may be involved in triggering amyloidosis. It may be possible that the ingestion of homologous or heterologous amyloid fibrils occurring in nature represents a factor in the initiation of amyloidosis. This possibility should be investigated further carefully. The characterization of AApoAII amyloidosis has proven helpful for identification of the genetics and epigenetics of amyloidosis, yielding results that are applicable to other protein-folding diseases as well.

## Acknowledgment

We thank Mr. S. Kametani at the General Research Laboratory of Shinshu University School of Medicine for valuable assistance with the EM studies.

## References

1. Westermark P: The pathogenesis of amyloidosis: understanding general principles. Am J Pathol 1998, 152:1125–1127
2. Booth DR, Sunde M, Bellotti V, Robinson CV, Hutchinson WL, Fraser PE, Hawkins PN, Dobson CM, Radford SE, Blake CC, Pepys MB: Instability, unfolding and aggregation of human lysozyme variants underlying amyloid fibrillogenesis. Nature 1997, 385:787–793
3. Glenner GG: Amyloid deposits and amyloidosis: the beta-fibrilloses. N Engl J Med 1980, 302:1283–1292
4. Xing Y, Higuchi K: Amyloid fibril proteins. Mech Ageing Dev 2002, 123:1625–1636
5. Higuchi K, Hosokawa M, Takeda T: Senescence-accelerated mouse. Methods Enzymol 1999, 309:674–686
6. Higuchi K, Yonezu T, Kogishi K, Matsumura A, Takeshita S, Kohono A, Matsushita T, Hosokawa M, Takeda T: Purification and characterization of a senile amyloid-related antigenic substance (apoSAS$_{SAM}$) from mouse serum. apoSAS$_{SAM}$ is an apoA-II apolipoprotein of mouse high density lipoproteins. J Biol Chem 1986, 261:12834–12840
7. Higuchi K, Matsumura A, Honma A, Takeshita S, Hashimoto K, Hosokawa M, Yasuhira K, Takeda T: Systemic senile amyloid in senescence-accelerated mice. A unique fibril protein demonstrated in tissues from various organs by the unlabeled immunoperoxidase method. Lab Invest 1983, 48:231–240
8. Higuchi K, Kitagawa K, Naiki H, Hanada K, Hosokawa M, Takeda T: Polymorphism of apolipoprotein A-II (apoA-II) among inbred strains of mice. Relationship between the molecular type of apoA-II and mouse senile amyloidosis. Biochem J 1991, 279:427–433
9. Naiki H, Higuchi K, Shimada A, Takeda T, Nakakuki K: Genetic analysis of murine senile amyloidosis. Lab Invest 1993, 68:332–337
10. Higuchi K, Wang J, Kitagawa K, Matsushita T, Kogishi K, Naiki H, Kitado H, Hosokawa M: Accelerated senile amyloidosis induced by amyloidogenic Apoa2 gene shortens the life span of mice but does not accelerate the rate of senescence. J Gerontol A Biol Sci Med Sci 1996, 51A:B295–B302
11. HogenEsch H, Niewold TA, Higuchi K, Tooten PC, Gruys E, Radl J: Gastrointestinal AAPOAII and systemic AA-amyloidosis in aged C57BL/Ka mice. Amyloid-type dependent effect of long-term immunosuppressive treatment. Virchows Arch B Cell Pathol Incl Mol Pathol 1993, 64:37–43
12. Gruys E, Tooten PJC, Kuijpers MHM: Swiss mice used for toxicity studies. Pulmonary amyloid indicates AApoAII. Lab Anim 1996, 30: 28–34
13. Shimizu K, Morita H, Niwa T, Maeda K, Shibata M, Higuchi K, Takeda T: Spontaneous amyloidosis in senile NSY mice. Acta Pathol Jpn 1993, 43:215–221
14. Prusiner SB: Prion diseases and the BSE crisis. Science 1991, 252: 1515–1522
15. Pan KM, Baldwin M, Nguyen J, Gasset M, Serban A, Groth D, Mehlhorn I, Huang Z, Fletterick RJ, Cohen FE, Prusiner SB: Conversion of alpha-helices into β-sheets features in the formation of the scrapie prion proteins. Proc Natl Acad Sci USA 1993, 90:10962–10966
16. Wickner RB, Edskes HK, Maddelein ML, Taylor KL, Moriyama H: Prions of yeast and fungi. Proteins as genetic material. J Biol Chem 1999, 274:555–558
17. Higuchi K, Kogishi K, Wang J, Chen X, Chiba T, Matsushita T, Hoshii Y, Kawano H, Ishihara T, Yokota T, Hosokawa M: Fibrilization in mouse senile amyloidosis is fibril conformation-dependent. Lab Invest 1998, 78:1535–1542
18. Naiki H, Higuchi K, Nakakuki K, Takeda T: Kinetic analysis of amyloid fibril polymerization in vitro. Lab Invest 1991, 65:104–110
19. Xing Y, Nakamura A, Chiba T, Kogishi K, Matsushita T, Li F, Guo Z, Hosokawa M, Mori M, Higuchi K: Transmission of mouse senile amyloidosis. Lab Invest 2001, 81:493–499
20. Xing Y, Nakamura A, Korenaga T, Guo Z, Yao J, Fu X, Matsushita T, Kogishi K, Hosokawa M, Kametani F, Mori M, Higuchi K: Induction of protein conformational change in mouse senile amyloidosis. J Biol Chem 2002, 277:33164–33169
21. Higuchi K, Naiki H, Kitagawa K, Kitado H, Kogishi K, Matsusita T, Takeda T: Apolipoprotein A-II gene and development of amyloidosis and senescence in a congenic strain of mice carrying amyloidogenic ApoA-II. Lab Invest 1995, 72:75–82
22. Inoue S, Kuroiwa M, Tan R, Kisilevsky RA: A high resolution ultrastructural comparison of isolated and in situ murine AA amyloid fibrils. Amyloid 1998, 5:99–110
23. Schagger H, Jagow G: Tricine-sodium dodecyl sulfate-polyacrylamide gel electrophoresis for the separation of proteins in the range from 1 to 100 kDa. Anal Biochem 1987, 166:368–379
24. Fu L, Matsuyama I, Chiba T, Xing Y, Korenaga T, Guo Z, Nakayama J, Mori M, Higuchi K: Extrahepatic expression of apolipoprotein A-II in mouse tissues: possible contribution to mouse senile amyloidosis. J Histochem Cytochem 2001, 49:739–748
25. Naiki H, Higuchi K, Hosokawa M, Takeda T: Fluorometric determination of amyloid fibrils in vitro using the fluorescent dye thioflavin T. Anal Biochem 1989, 177:244–249
26. Soto C, Sigurdsson EM, Morelli L, AsokKumar R, Castaño EM, Frangione B: β-sheet breaker peptides inhibit fibrillogenesis in a rat brain model of amyloidosis: implications for Alzheimer's therapy. Nat Med 1998, 4:822–826
27. Osherovich LZ, Weissman JS: Multiple Gln/Asn-rich prion domains confer susceptibility to induction of the yeast [PSI(+)] prion. Cell 2001, 106:183–194
28. Sakashita N, Ando Y, Jinnouchi K, Yoshimatsu M, Terazaki H, Obayashi K, Takeya M: Familial amyloidotic polyneuropathy (ATTR Val30Met) with widespread cerebral amyloid angiopathy and lethal cerebral hemorrhage. Pathol Int 2001, 51:476–480
29. Lobato L: Portuguese-type amyloidosis (transthyretin amyloidosis, ATTR V30M). J Nephrol 2003, 16:438–442
30. Nichols WC, Gregg RE, Brewer Jr HB, Benson MD: A mutation in apolipoprotein A-I in the Iowa type of familial amyloidotic polyneuropathy. Genomics 1990, 8:318–323
31. Booth DR, Tan SY, Booth SE, Tennent GA, Hutchinson WL, Hsuan JJ, Totty NF, Truong O, Soutar AK, Hawkins PN, Bruguera M, Caballeria J, Sole M, Campistol JM, Pepys MB: Hereditary hepatic and systemic amyloidosis caused by a new deletion/insertion mutation in the apolipoprotein AI gene. J Clin Invest 1996, 97:2714–2721
32. Hamidi Asl L, Liepnieks JJ, Hamidi Asl K, Uemichi T, Moulin G, Desjoyaux E, Loire R, Delpech M, Grateau G, Benson MD: Hereditary amyloid cardiomyopathy caused by a variant apolipoprotein A1. Am J Pathol 1999, 154:221–227
33. Ikeda S, Nakazato M, Ando Y, Sobue G: Familial transthyretin-type amyloid polyneuropathy in Japan: clinical and genetic heterogeneity. Neurology 2002, 58:1001–1007
34. Jacobson DR, McFarlin DE, Kane I, Buxbaum JN: Transthyretin Pro55, a variant associated with early-onset, aggressive, diffuse amyloidosis with cardiac and neurologic involvement. Hum Genet 1992, 89:353–356
35. Takahashi K, Yi S, Kimura Y, Araki S: Familial amyloidotic polyneuropathy type 1 in Kumamoto, Japan: a clinicopathologic, histochemical, immunohistochemical, and ultrastructural study. Hum Pathol 1991, 22:519–527
36. Ionescu-Zanetti C, Khurana R, Gillespie JR, Petrick JS, Trabachino LC, Minert LJ, Carter SA, Fink AL: Monitoring the assembly of Ig

light-chain amyloid fibrils by atomic force microscopy. Proc Natl Acad Sci USA 1999, 39:13175–13179
37. Harper JD, Wong SS, Lieber CM, Lansbury PT: Observation of metastable Aβ amyloid protofibrils by atomic force microscopy. Chem Biol 1997, 4:119–125
38. Quintas A, Vaz DC, Cardoso I, Saraiva MJ, Brito RM: Tetramer dissociation and monomer partial unfolding precedes protofibril formation in amyloidogenic transthyretin variants. J Biol Chem 2000, 276: 27207–27213
39. Kaplan B, Vidal R, Kumar A, Ghiso J, Frangione B, Gallo G: Amino-terminal identity of co-existent amyloid and non-amyloid immunoglobulin kappa light chain deposits. A human disease to study alterations of protein conformation. Clin Exp Immunol 1997, 110:472–478
40. Sousa MM, Cardoso I, Fernandes R, Guimaraes A, Saraiva MJ: Deposition of transthyretin in early stages of familial amyloidotic polyneuropathy: evidence for toxicity of nonfibrillar aggregates. Am J Pathol 2001, 159:1993–2000
41. Sousa MM, Fernandes R, Palha JA, Taboada A, Vieira P, Saraiva MJ: Evidence for early cytotoxic aggregates in transgenic mice for human transthyretin Leu55Pro. Am J Pathol 2002, 161:1935–1938
42. Teng MH, Yin JY, Vidal R, Ghiso J, Kumar A, Rabenou R, Shah A, Jacobson DR, Tagoe C, Gallo G, Buxbaum J: Amyloid and nonfibrillar deposits in mice transgenic for wild-type human transthyretin: a possible model for senile systemic amyloidosis. Lab Invest 2001, 81:385–396
43. Lundmark K, Westermark GT, Nystrom S, Murphy CL, Solomon A, Westermark P: Transmissibility of systemic amyloidosis by a prion-like mechanism. Proc Natl Acad Sci USA 2002, 99:6979–6984
44. Sigurdsson EM, Wisniewski T, Frangione B: Infectivity of amyloid diseases. Trends Mol Med 2002, 8:411–413
45. Hoshino M, Katou H, Hagihara Y, Hasegawa K, Naiki H, Goto Y: Mapping the core of the β2-microglobulin amyloid fibril by H/D exchange. Nat Struct Biol 2002, 9:332–336
46. Prusiner SB: Shattuck lecture—neurodegenerative diseases and prions. N Engl J Med 2001, 344:1516–1526
47. Santoso A, Chien P, Osherovich LZ, Weissman JS: Molecular basis of a yeast prion species barrier. Cell 2000, 100:277–288
48. Prusiner SB, Scott MR, DeArmond SJ, Cohen FE: Prion protein biology. Cell 1998, 93:337–348
49. Chien P, Weissman JS: Conformational diversity in a yeast prion dictates its seeding specificity. Nature 2000, 410:223–227
50. Cui D, Kawano H, Takahashi M, Hoshii Y, Setoguchi M, Gondo T, Ishihara T: Acceleration of murine AA amyloidosis by oral administration of amyloid fibrils extracted from different species. Pathol Int 2002, 52:40–45
51. Ganowiak K, Hultman P, Engstrom U, Gustavsson A, Westermark P: Fibrils from synthetic amyloid-related peptides enhance development of experimental AA-amyloidosis in mice. Biochem Biophys Res Commun 1994, 199:306–312
52. Kisilevsky R, Lemieux L, Boudreau L, Yang DS, Fraser P: New clothes for amyloid enhancing factor (AEF): silk as AEF. Amyloid 1999, 6:98–106
53. Maddelein ML, Dos Reis S, Duvezin-Caubet S, Coulary-Salin B, Saupe SJ: Amyloid aggregates of the HET-s prion protein are infectious. Proc Natl Acad Sci USA 2002, 99:7402–7407
54. Chapman MR, Robinson LS, Pinkner JS, Roth R, Heuser J, Hammar M, Normark S, Hultgren SJ: Role of Escherichia coli curli operons in directing amyloid fiber formation. Science 2002, 295:851–855
55. Derkatch IL, Bradley ME, Hong JY, Liebman SW: Prions affect the appearance of other prions: the story of [PIN(+)]. Cell 2001, 106:171–182